Letter

Low-frequency cryocoolers are compressed inefficiently

Ryan Snodgrass[1,2,*] Vincent Kotsubo[1,2] Jens Höhne[3] and Joel Ullom[1,2]

[1] *National Institute of Standards and Technology, Boulder, Colorado 80305, USA*

[2] *Department of Physics, University of Colorado Boulder, Boulder, Colorado 80309, USA*

[3] *Pressure Wave Systems GmbH, Hochstr. 21A, 82024 Taufkirchen, Germany*

(Received 19 September 2025; revised 25 November 2025; accepted 3 February 2026; published 10 March 2026)

Millikelvin refrigerators are enabling tools for many fields of modern science, including quantum information processing. They are typically precooled to 4 K by low-frequency pulse-tube refrigerators, which perform a thermodynamic cycle based on compressing and expanding helium gas. Although the efficiency of these refrigerators is known to be poor, only the loss mechanisms that occur near the cold end have been sufficiently studied and characterized. Here, we combine thermoacoustic calculations with measurements from a commercial pulse-tube refrigerator to determine the efficiency of the generation and transmission of acoustic power, which the refrigerator uses to provide cooling. We find that electrical power consumed by the compressor is converted to acoustic power at a rate of only 0.24, while acoustic power is transmitted through the refrigerator at a comparatively high efficiency of 0.66. The compression process therefore dominates the portion of the system efficiency that is not limited by fluid and material properties. To show that more efficient compression is possible, we also performed measurements on a new metal-bellows compressor that converts electricity to acoustic power at factors up to 0.43. Our results show that low temperatures may be achievable with two or perhaps even three times less electricity.

DOI: 10.1103/jcb9-j97v

Introduction. Millikelvin temperatures are required for a large variety of modern science and technology, including state-of-the-art quantum processors [1,2]. Such low temperatures are reached with dilution refrigerators or adiabatic demagnetization refrigerators, although these systems must first be precooled to around 4 K. This task was once achieved using liquid nitrogen and helium, but it is now almost always accomplished with low-frequency Gifford-McMahon (GM)-type pulse-tube refrigerators (PTRs).

This class of cryocooler has many advantages. They can be purchased relatively inexpensively from multiple manufacturers, and their users need only press a single button to cool payloads to extremely low temperatures (2.5 K is routine with small heat loads). They are closed systems, so they are filled with high-pressure helium-4 just once. The compressors that drive these cryocoolers supply contamination-free gas, even though they are oil lubricated [3,4], and they can be placed many meters from the cryocooler, which eases cryostat construction and reduces mechanical vibrations at the cold end. The absence of moving parts in the refrigerator body further reduces vibrations, an advantage that has proven critical for cooling quantum electronics.

The major drawback of GM-type PTRs is poor efficiency. Typically, 10 kW of electrical power is consumed to produce 1 W of cooling power at 4 K (about 1% of the Carnot limit). Cryocooler efficiency is most often defined by how much cooling power is produced and how much electricity is consumed; however, this definition does not provide any guidance on how to make improvements. In this study, we take a different perspective, focusing on two steps that must occur before the refrigerator can produce cooling power. The first step is the generation of acoustic power (also called fluid power) at the refrigerator inlet. Electricity is consumed by the compressor to generate mass flow, which compresses and expands the gas within the coldhead. The second step is the transmission of acoustic power through the refrigerator, from inlet to thermodynamic core. This core consists of a regenerator, a thermal buffer tube (also called pulse tube), and a heat exchanger; in the ideal case, it converts all of the acoustic power transmitted to the cold end into cooling power.

Through a combination of calculations and measurements performed on a widely used commercial PTR, we show that the generation of acoustic power from electricity limits the performance of the system much more than the transmission of acoustic power through the coldhead. This is a significant result because it identifies the clearest path toward improving the overall efficiency of these systems.

*Contact author: ryan.snodgrass@nist.gov

Published by the American Physical Society under the terms of the Creative Commons Attribution 4.0 International license. Further distribution of this work must maintain attribution to the author(s) and the published article's title, journal citation, and DOI.

Although there are other loss mechanisms that contribute to poor overall efficiency in GM-type cryocoolers, they are largely unavoidable, being limited by the real-fluid properties of helium at very low temperatures and the limited heat capacity of state-of-the-art regenerator materials [5]. The losses associated with the generation of acoustic power, however, could be markedly decreased by avoiding a fundamentally flawed compression process.

The gas in GM-type cryocoolers is compressed and expanded by alternately connecting the coldhead to high- and low-pressure reservoirs that are created by a scroll compressor running at 50 or 60 Hz. A rotary valve spinning near 1 Hz is used to change the reservoir to which the coldhead is connected; however, one of the fundamental mechanisms of exergy destruction is mass flowing across a pressure difference. Since the coldhead is connected to the high-pressure reservoir when it is at low pressure and is connected to the low-pressure reservoir when it is at high pressure, GM-type compression is inherently lossy. GM-type cryocoolers have used these compressors since at least 1970 [3,6], employing hardware that was originally developed for air-conditioning units. More than half a century later, it is time to consider whether better compression methods are available or can be developed.

As far as we are aware, there have been no complete measurements characterizing the efficiency of either the generation or transmission of acoustic power through these systems. In 2001, an analysis of GM-type cryocoolers using idealized waveforms hypothesized that the rotary valve transmits only about half of the exergy it receives from the compressor [7], but no validating measurements followed. Some studies have used numerical tools to investigate the efficiency of rotary valves for GM cryocoolers [8,9] and GM-type PTRs [10]; however, these studies concluded that rotary-valve losses can largely be attributed to the flow resistance of the valve and the leakage through it. In contrast, our experimental measurements show insignificant leakage, and we do not believe that decreasing flow resistance can significantly improve valve efficiency. Since the coldhead is alternated between two pressure reservoirs, exergy destruction would occur even with zero flow resistance.

In addition to quantifying the efficiency of acoustic power generation and transmission in a commercial 4 K PTR, in this study, we also measure the performance of a new compressor constructed from metal bellows, demonstrating that superior compression methods are available.

System efficiency may not be the foremost concern for some cryostat users, but we foresee it becoming increasingly important. Cryostats with millikelvin refrigerators require three-phase power and large amounts of cooling water just to run the 4 K precooler. Many institutions support tens of cryostats that are almost always in operation, and applications with limited access to utilities (e.g., balloon [11,12] and remote experiments [13]) or with many cryostats spread across large distances (future quantum information networks [14]) would greatly benefit from smaller and more efficient compressors.

Acoustic power and exergy. To characterize the efficiency of energy conversion at locations between the wall outlet and cryocooler cold end, we will use two measures of power: acoustic power and exergy.

The generation of acoustic power and its transmission to the cold end of the refrigerator is our primary concern since it is converted into cooling power by the thermodynamic core. Intuitively, acoustic power can be understood as the rate of work exerted by an imaginary piston placed in the flow. It is typically defined in the thermoacoustic framework [15] for systems with sinusoidal waves at low amplitudes, e.g., small pressure oscillations compared to the mean pressure. Unfortunately, GM-type cryocoolers do not operate under these assumptions: waveforms are not sinusoidal, and there are large pressure and density oscillations. We have therefore generalized the concept of acoustic power, a task that has not previously been completed. A full description can be found in Sec. A of the Supplemental Material [16], but the result is that the generalized acoustic power is

$$\dot{E} = \overline{(p - \overline{p})U_p}, \tag{1}$$

where p is pressure and the imaginary piston flow rate $U_p \neq \dot{m}/\rho$, the measured volumetric flow rate ($\dot{m}$ is the mass flow rate and ρ is the gas density). Instead, U_p can be found using Eq. (S2) in the Supplemental Material [16]. The overline represents the cycle mean.

The generation of acoustic power can be more robustly analyzed by separately considering the compressor, helium hoses, and rotary valve. Unlike the refrigerator, these components operate at nominally steady pressures ($p - \overline{p} \approx 0$), so acoustic power cannot be used to assess their efficiency. Instead, exergy analysis can be used. Exergy is the available mechanical power of a flow stream that is not in thermal and mechanical contact with its environment. It is equal to the mass flow rate multiplied by the specific exergy [17]. The mean exergy is

$$\dot{X} = \overline{\dot{m}[h^\circ - h_0^\circ - T_0(s - s_0)]}, \tag{2}$$

where the methalpy $h^\circ = h + \frac{1}{2}u^2 + gz$ is the sum of the enthalpy, kinetic energy, and gravitational potential energy (all per unit mass), and s is the entropy (per unit mass). In our calculations, we neglected the gravitational potential but included kinetic energy, although its contribution was small (0.2% of $\dot{X}$). The restricted dead state (subscript 0) was evaluated at $\overline{p}$ and 280 K (the temperature T of the water cooling the compressor). Net exergy was calculated by summing $\dot{X}$ at different locations; e.g., the net exergy of the compressor $\dot{X}_c = \dot{X}_{\text{high}} + \dot{X}_{\text{low}}$, with $\dot{m}$ taken as positive on the high side and negative on the low side.

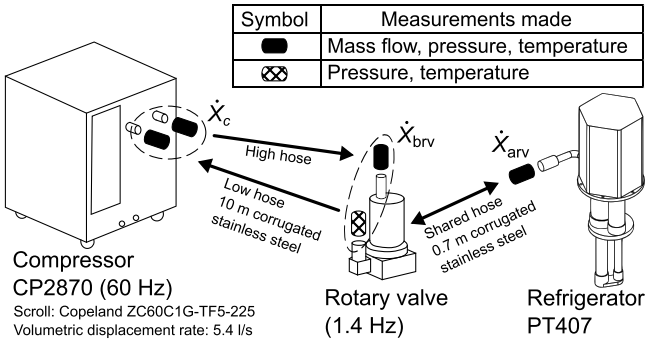


FIG. 1. Experimental overview. Two flow meters at the high and low sides of the compressor give the net exergy from the compressor $\dot{X}_c$. Two sensors after the helium hoses but before the rotary valve give the net exergy there $\dot{X}_{brv}$. A single flow meter mounted at the inlet of the PTR gives the exergy after the rotary valve $\dot{X}_{arv}$.

Acoustic power and exergy were calculated using measurements of $\dot{m}$, p, and T at the locations shown in Fig. 1; methodological details are provided in Sec. B.1 of the Supplemental Material [16]. The PTR studied was a Cryomech PT407 paired with CP2870 compressor.

Efficiency measurements. The mass flows, pressures, and temperatures at the locations shown in Fig. 1 are plotted under normal operating conditions (1.4 Hz rotary-valve frequency and no heat applied to the cold ends) in Fig. 2. Gas properties were calculated using the measured p and T. In addition to the locations shown in Fig. 1, the pressure was also measured inside the PTR by transducers installed on both sides of the main orifices.

Data from Fig. 2 were used to calculate component efficiencies, which are summarized in Table I. The efficiency of the scroll compressor was calculated as the net exergy produced by the compressor $\dot{X}_c$ divided by its electrical power draw: 0.44. A study of scroll compressors made by other manufacturers measured efficiencies up to about 0.46 [18]. The efficiency of the helium hoses and associated fittings was calculated as the net exergy at the rotary-valve inputs $\dot{X}_{brv}$ divided by $\dot{X}_c$: 0.93. The efficiency of the rotary valve was measured by dividing the net exergy at the PTR inlet $\dot{X}_{arv}$ by $\dot{X}_{brv}$: 0.59. We measured little to no leakage through the rotary valve (see Sec. C.4 of the Supplemental Material [16]); although this is a potential loss mechanism, it does not appear to impact these commercial systems. The $\dot{E}$ measured inside the ambient end of the PTR divided by the electricity input to the compressor was 0.24.

TABLE I. Efficiency of a PT407 paired with a CP2870 compressor, under steady-state conditions. A more detailed version of this table can be found in Sec. C.1 of the Supplemental Material [16].

Component	Efficiency
Scroll compressor	0.44
Helium hoses and fittings	0.93
Rotary valve	0.59
Process	
Electric to acoustic power conversion	0.24
Acoustic power transmission in coldhead	0.66

As discussed in the Introduction, we are concerned with both the generation of $\dot{E}$ from electricity and the transmission of $\dot{E}$ through the coldhead; we now discuss this latter process. The maximum amount of $\dot{E}$ at the cold end of a PTR is the inlet $\dot{E}$ multiplied by the ratio of the gas densities at the ambient and cold ends. This calculation assumes a lossless PTR with a single regenerator and no bypass paths; however, in this cryocooler, some $\dot{E}$ flows through bypass paths (because it uses the double-inlet geometry [19]), some flows into the first-stage buffer tube (the PT407 has two cold stages, and this flow provides cooling at a relatively warm first-stage temperature), and some is lost to viscosity. Although we were unable to directly measure

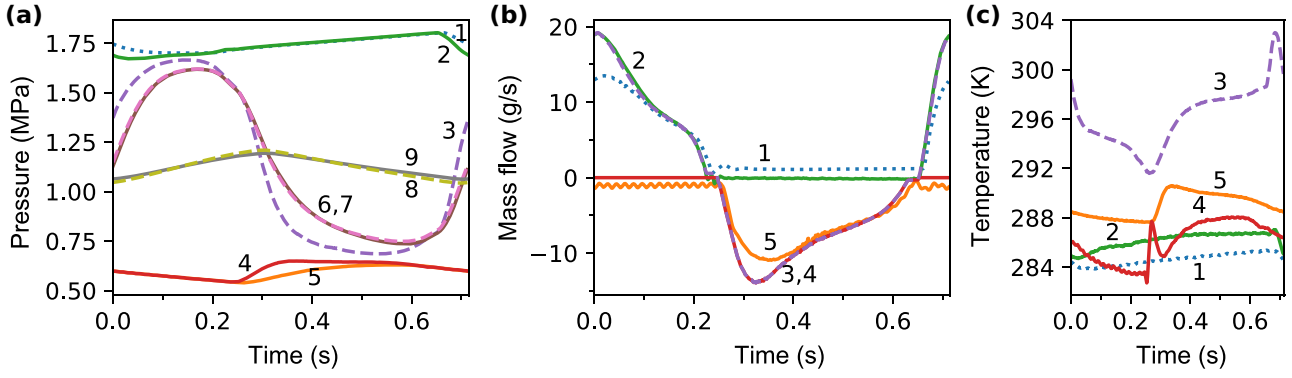


FIG. 2. (a) Pressures, (b) mass flows, and (c) gas temperatures in a PT407 under normal operating conditions. Positive mass flow is into the coldhead and away from the compressor. (1) High side of compressor, (2) high side of rotary valve, (3) PTR inlet, (4) low side of rotary valve, (5) low side of compressor, (6),(7) first- (solid) and second-stage (dashed) junction (where the main orifice, buffer tube, and bypass meet), (8) second-stage reservoir, (9) first-stage reservoir.

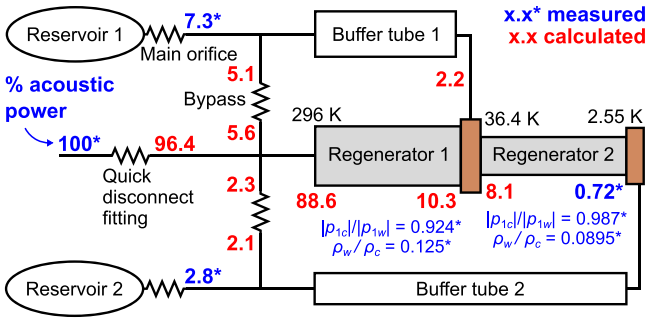


FIG. 3. Distribution of acoustic power inside a PT407 under normal operating conditions. The ratio of the pressure amplitudes at the cold and warm ends of each regenerator is $|p_{1c}|/|p_{1w}|$, while ρ_w/ρ_c is the ratio of the gas densities.

$\dot{E}$ at the coldest heat exchanger in this PT407, we previously calculated it using cooling-power measurements and the unique behavior of regenerators in the real-fluid regime [5]. Additional details on this topic are provided in Sec. B.2 of the Supplemental Material [16]. The ratio of the actual cold-end $\dot{E}$ to the maximum theoretical cold-end $\dot{E}$ for an ideal PTR is the efficiency of acoustic power transmission through the coldhead: 0.66.

We were also able to identify which mechanisms decrease the efficiency of acoustic power transmission by calculating $\dot{E}$ everywhere in the PTR (Fig. 3), as explained in Sec. B.3 of the Supplemental Material [16]. We are not aware of a similar measurement elsewhere in the literature, although it indicates multiple strategies for improving these refrigerators. Inlet $\dot{E}$ drops by approximately 4% in the quick-disconnect fitting installed at the PTR entrance; decreasing its flow resistance would boost cooling power at both stages. Figure 3 also shows nearly an 8% decrease to $\dot{E}$ due to the pressure drop through the first-stage regenerator; this inefficiency could be addressed through regenerator design. At the first-stage heat exchanger, $\dot{E}$ is split between the first-stage buffer tube and the second-stage regenerator; however, this distribution could be modified (by tuning the main orifices) to provide more or less cooling at the two stages.

About 8% of the $\dot{E}$ that makes it through the refrigerator inlet is sent to the two bypass paths. Although this flow does not directly contribute to cooling either stage, it has a net positive impact. First, it helps to pressurize the gas in the buffer tubes without increasing the viscous loss in the regenerators. Second, the bypass paths create the toroidal geometry necessary for Gedeon streaming [20], which serves a critical function: absorbing the loss of the second-stage buffer tube with the excess cooling power of the 4 K regenerator [5].

A typical cooldown of the PTR (Fig. 4) provides more insight into the efficiency of the compressor and rotary valve. GM-type PTRs are inherently inefficient during cooldown because of poor impedance matching

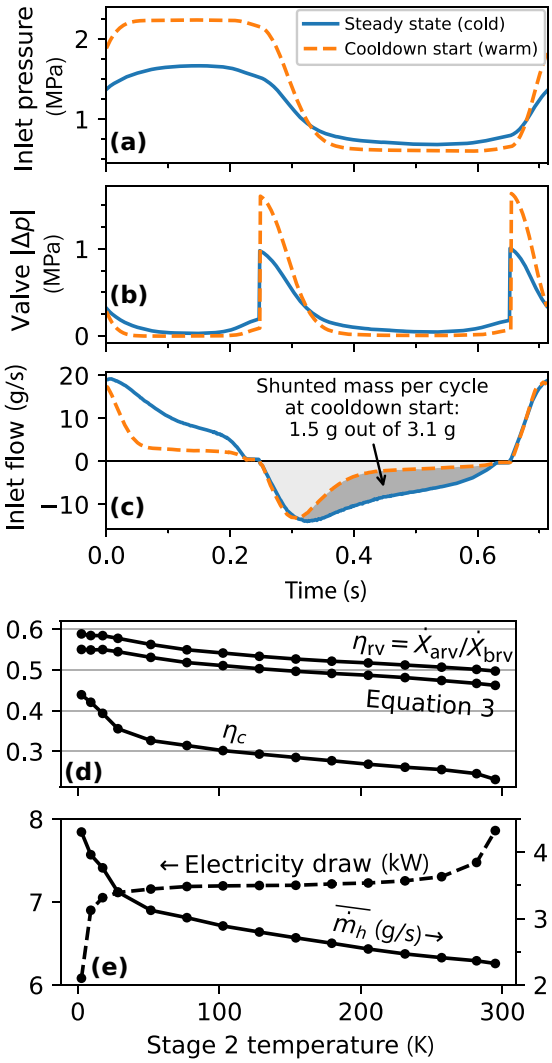


FIG. 4. Measurements during a typical PT407 cooldown. (a) Inlet pressure, (b) absolute pressure difference across the rotary valve, and (c) inlet flow rate before and after cooldown. (d) Rotary-valve efficiency η_{rv}, compressor efficiency η_c, and (e) electrical power draw and mean mass flow rate from the compressor at many temperatures between ambient and 2.55 K.

between the coldhead and the compressor, as we previously explained [21]. Near ambient temperature, a large pressure difference develops between the high and low sides of the compressor, opening a relief valve and shunting (wasting) mass flow. The shunted mass was measured indirectly by comparing the inlet mass flow rates before and after cooldown: the area between these curves shows that almost half of the mass flow supplied by the compressor is wasted at the start of cooldown [Fig. 4(c)]. The compressor efficiency η_c increases from 23% to 44% during cooldown, largely because less mass is shunted but also because electricity draw decreases by almost 2 kW during cooldown. This latter observation is likely explained by the decrease to the high compressor pressure (see Sec. C.5 of the Supplemental Material [16]).

TABLE II. Power-conversion efficiency for four types of cryocooler compressor.

Compressor	Frequency (Hz)	Refrigerator type	Electric-to-acoustic-power efficiency	Reference
Scroll/rotary valve	1.4	GM-type PTR	0.24	This work
Metal bellows	1.2	GM (single)	0.34	This work
		GM (double)	0.43	
Resonant linear	40 to 120	Stirling-type PTR	0.70 to 0.80	[25–29]
Metal diaphragm	30 to 60	Stirling-type PTR	0.72	[30]

The rotary-valve efficiency η_{rv} increases from 50% to 59% during cooldown. This increase in η_{rv} can be explained by our analysis of rotary-valve efficiency, the details of which are given in Sec. B.4 of the Supplemental Material [16]. The primary result of that analysis is that for GM-type cryocoolers, the rotary-valve efficiency is

$$\eta_{\mathrm{rv}} \simeq \overline{\dot{m}\ln p}\,\Big/\,\overline{\dot{m}_h}\ln\frac{p_h}{p_l}, \tag{3}$$

where p_h and p_l are the steady pressures on the high and low sides of the valve, and $\overline{\dot{m}_h}$ is the mean flow rate supplied by the compressor. The denominator of Eq. (3) is determined by the sizing of the compressor and coldhead and does not present a path toward optimizing η_{rv}; however, the numerator shows that η_{rv} is maximized if mass flows into the coldhead when it is at high pressure and flows out of the coldhead when it is at low pressure; in other words, mass should flow when there is minimal pressure difference across the valve. At cooldown start, the majority of mass flows in bursts when the pressure difference across the valve is large [dashed lines in Figs. 4(b) and 4(c) near 0.3 s]. After cooldown, $\dot{m}$ stays at higher levels after the initial burst and is transferred across a smaller pressure difference [solid lines in Figs. 4(b) and 4(c) between 0.4 and 0.6 s], decreasing exergy destruction. In Sec. B.4 of the Supplemental Material [16], we also show that the maximum rotary-valve efficiency is $\pi/4 \approx 0.79$; however, sinusoidal waves need to be assumed to reach this solution—a mediocre approximation for real GM-type cryocoolers.

A metal-bellows compressor, developed by Pressure Wave Systems GmbH and manufactured by attocube systems GmbH, demonstrates one path toward more-efficient compression of GM-type cryocoolers. This compressor uses a gear pump and two metal bellows to move gas in and out of the coldhead. The compressor and coldhead are directly connected, avoiding rotary-valve losses. We measured the efficiency of this system with the same flow meters used to inspect the PT407. When one GM cryocooler was connected to the compressor, electricity was converted to acoustic power at a factor of 0.34, and with two GM cryocoolers connected to the compressor, the conversion efficiency increased to 0.43. Details of the compressor and experiment are given in Sec. C.2 of the Supplemental Material [16]. Unfortunately, this compressor does not supply enough mass flow to compress the PT407 studied here, nor the larger PTRs that are typically used to precool commercial dilution refrigerators. The mean flow supplied to the PT407 from the scroll compressor was 4.3 g/s, while the mean flow supplied by the metal-bellows compressor was only 0.7 g/s. It is not yet known if much larger bellows compressors are viable; entirely different compressor architectures should also be considered.

Outlook. Gifford-McMahon-type 4 K PTRs operate near 1% of the Carnot limit. Multiple factors contribute to this poor efficiency. Over 90% of the cooling power that could be available is instead lost to the real-fluid effects of helium and the finite heat capacity of state-of-the-art regenerator materials [5]. Although these losses can be offset by using regenerator cooling [5,22,23], they cannot be avoided, as they result from the thermophysical properties of helium. In contrast to those losses, the inefficiencies quantified in this work are largely unnecessary. For the first time, we have identified that acoustic power is transmitted at relatively high efficiency through these refrigerators, but that only one quarter of the electricity input to the compressor is converted into acoustic power.

High-frequency PTRs provide an interesting point of comparison. These cryocoolers usually provide cooling at warmer temperatures, only reaching 4 K through complicated means (e.g., using helium-3 as the working fluid [24]); however, they typically convert electricity to acoustic power at rates between 0.7 and 0.8 (Table II). If low-frequency, GM-type 4 K cryocoolers were compressed at this efficiency, three times less electricity would be required. It may then be feasible to run millikelvin refrigerators without three-phase power and cooling water, drastically increasing the accessibility of low-temperature science.

There are challenges to developing high-efficiency compressors for low-frequency cryocoolers. To generate large acoustic powers, low-frequency cryocoolers operate at high pressure amplitudes and therefore require the compressor to displace large amounts of gas during each cycle. This gas should also be compressed isothermally. GM-type compressors overcome these challenges by using small, oil-flooded compression spaces that are displaced at a frequency much higher than the cryocooler frequency.

Another challenge is recovering the work of compression. It is straightforward to design a linear compressor with resonant frequency near the powerline frequency, but large masses or long strokes are required for resonant frequencies near 1 Hz [31]. Storing energy in a flywheel is also impractical at 1 Hz.

Although there are significant challenges for compressing cryocoolers at frequencies near 1 Hz, the metal-bellows compressor characterized in this study suggests that large gains in efficiency are possible. Further work in compressor design is needed to bridge the gap in efficiency between low-frequency and high-frequency PTRs; however, it is the clearest path toward increasing the accessibility of temperatures 4 K and below.

Acknowledgments. We acknowledge support from the Professional Research Experience Program between the University of Colorado Boulder and NIST under Award No. 70NANB18H006. The manuscript is a contribution of NIST and not subject to copyright. Certain equipment, instruments, or materials are identified in this paper to specify the experimental procedure adequately. Such identification is not intended to imply recommendation or endorsement by NIST, nor is it intended to imply that the materials or equipment identified are necessarily the best available for the purpose. We acknowledge guidance and advice on the topic of this manuscript from Gregory Swift and Ray Radebaugh.

R.S.: conceptualization, methodology, investigation, data curation, writing, and visualization. V.K.: conceptualization, methodology, and supervision. J.H.: investigation and resources. J.U.: supervision, funding acquisition, and writing.

J.H. is the founder of Pressure Wave Systems GmbH, developer of the metal-bellows compressor.

Data availability. The data that support the findings of this article are contained within the main manuscript and Supplemental Material. Raw data are available from the authors upon reasonable request.

[1] F. Arute, K. Arya, R. Babbush, D. Bacon, J. C. Bardin, R. Barends, R. Biswas, S. Boixo, F. G. S. L. Brandao, D. A. Buell *et al.*, Quantum supremacy using a programmable superconducting processor, Nature **574**, 505 (2019).

[2] R. Acharya, D. A. Abanin, L. Aghababaie-Beni, I. Aleiner, T. I. Andersen, M. Ansmann, F. Arute, K. Arya, A. Asfaw, N. Astrakhantsev *et al.*, Quantum error correction below the surface code threshold, Nature **638**, 920 (2025).

[3] R. C. Longsworth, Helium compressor for GM and pulse-tube expanders, in *AIP Conference Proceedings* (2002), Vol. 613, pp. 691–698.

[4] C. Wang, Z. Zhao, and J. Wu, Nearly isothermal compression characteristics of the helium oil-flooded scroll compressor, Appl. Therm. Eng. **251**, 123597 (2024).

[5] R. Snodgrass, G. Swift, J. Ullom, and S. Backhaus, Intermediate cooling from pulse tube refrigerator regenerators operating in the real-fluid regime, Cryogenics **132**, 103685 (2023).

[6] R. C. Longsworth, A modified Solvay-Cycle cryogenic refrigerator, in *Advances in Cryogenic Engineering* (1971), pp. 195–204.

[7] Y. L. Ju, Thermodynamic analysis of GM-type pulse tube coolers, Cryogenics **41**, 513 (2001).

[8] Q. Zhao, B. Wang, W. Chao, J. Cheng, Y. Zhang, H. Zhang, and Z. Gan, Numerical simulation and exergy analysis of a single-stage GM cryocooler, Heliyon **9**, e18479 (2023).

[9] T. Gao, C. Wu, X. Chen, X. Zhi, and L. Qiu, Numerical simulation and loss analysis on a two-stage GM cryocooler working at liquid helium temperatures, Cryogenics **150**, 104145 (2025).

[10] D. Liu, M. Dietrich, G. Thummes, and Z. Gan, Numerical simulation of a GM-type pulse tube cryocooler system: Part II. Rotary valve and cold head, Cryogenics **81**, 100 (2017).

[11] P. A. R. Ade, M. Amiri, S. J. Benton, A. S. Bergman, R. Bihary, J. J. Bock, J. R. Bond, J. A. Bonetti, S. A. Bryan, H. C. Chiang *et al.*, A constraint on primordial b-modes from the first flight of the Spider balloon-borne telescope, Astrophys. J. **927**, 174 (2022).

[12] F. Shirazi, M. A. Hossen, D. Becker, D. Schmidt, D. Swetz, D. Bennett, D. Braun, E. Gau, F. Kislat, J. Gard *et al.*, The 511-CAM mission: A pointed 511 keV gamma-ray telescope with a focal plane detector made of stacked transition edge sensor microcalorimeter arrays, J. Astron. Telesc. Instrum. Syst. **9**, 024006 (2023).

[13] N. Zhu, T. Bhandarkar, G. Coppi, A. M. Kofman, J. L. Orlowski-Scherer, Z. Xu, S. Adachi, P. Ade, S. Aiola, J. Austermann *et al.*, The Simons Observatory Large Aperture Telescope Receiver, Astrophys. J. Suppl. Ser. **256**, 23 (2021).

[14] M. K. Bhaskar, R. Riedinger, B. Machielse, D. S. Levonian, C. T. Nguyen, E. N. Knall, H. Park, D. Englund, M. Lončar, D. D. Sukachev *et al.*, Experimental demonstration of memory-enhanced quantum communication, Nature **580**, 60 (2020).

[15] G. W. Swift, *Thermoacoustics: A Unifying Perspective for Some Engines and Refrigerators* (Springer International Publishing AG, Cham, Switzerland, 2017), 2nd ed.

[16] See Supplemental Material at http://link.aps.org/supplemental/10.1103/jcb9-j97v for description of generalized acoustic power, methods, and supplementary results. The Supplemental Material also includes Refs. [32–37].

[17] A. Bejan, *Advanced Engineering Thermodynamics* (John Wiley & Sons, Inc., New York, NY, 1997).

[18] D. Liu, M. Dietrich, G. Thummes, and Z. Gan, Numerical simulation of a GM-type pulse tube cryocooler system: Part I. Characterization of compressors, Cryogenics **81**, 8 (2017).

[19] S. Zhu, P. Wu, and Z. Chen, Double inlet pulse tube refrigerators: An important improvement, Cryogenics **30**, 514 (1990).

[20] D. Gedeon, DC gas flows in Stirling and pulse tube cryocoolers, Cryocoolers **9**, 385 (1997).

[21] R. Snodgrass, V. Kotsubo, S. Backhaus, and J. Ullom, Dynamic acoustic optimization of pulse tube refrigerators for rapid cooldown, Nat. Commun. **15**, 3386 (2024).

[22] R. Snodgrass, J. Ullom, and S. Backhaus, Optimal absorption of distributed and conductive heat loads with cryocooler regenerators, IOP Conf. Ser.: Mater. Sci. Eng. **1240**, 012131 (2022).
[23] R. Snodgrass, V. Kotsubo, J. Ullom, and S. Backhaus, Leveraging real fluid effects as a tool for power flow measurements in 4 K cryocooler regenerators, Cryocoolers **21**, 315 (2021).
[24] T. Nast, J. Olson, P. Champagne, J. Mix, B. Evtimov, E. Roth, A. Collaco, J. G. Weisend, J. Barclay, S. Breon *et al.*, Development of a 4.5 K pulse tube cryocooler for superconducting electronics, in *AIP Conference Proceedings* (2008), Vol. 985, pp. 881–886.
[25] Y. Chao, Q. Zhao, Y. Guo, B. Wang, C. Xiong, H. Li, and Z. Gan, Acoustic power measurement of linear compressors, Cryogenics **96**, 10 (2018).
[26] W. Dai, E. Luo, X. Wang, and Z. Wu, Impedance match for Stirling type cryocoolers, Cryogenics **51**, 168 (2011).
[27] L. Y. Wang, Z. H. Gan, Y. X. Guo, B. Wang, and S. H. Wang, Electric-mechanical-acoustic coupling characteristics for pulse tube cryocoolers, Cryocoolers **19**, 193 (2016).
[28] Q. Cao, Z. H. Gan, G. J. Liu, Z. P. Li, Y. Z. Wu, L. M. Qiu, and J. M. Pfotenhauer, Theoretical and experimental study on a pulse tube cryocooler driven with a linear compressor, Cryocoolers **15**, 149 (2009).
[29] A. Zhang, Y. Wu, S. Liu, H. Zhu, Y. Zeng, Z. Jiang, and A. Kan, Effect of impedance on a compressor driving pulse tube refrigerator, Appl. Therm. Eng. **124**, 688 (2017).
[30] A. J. Caughley, D. J. Haywood, C. Wang, J. G. Weisend, J. Barclay, S. Breon, J. Demko, M. DiPirro, J. P. Kelley, P. Kittel *et al.*, A low cost pressure wave generator using diaphragms, in *AIP Conference Proceedings* (2008), Vol. 985, pp. 1122–1129.
[31] E. Marquardt, R. Radebaugh, and P. Kittel, Design equations and scaling laws for linear compressors with flexure springs, Cryocoolers **7**, 783 (1993).
[32] A. D. Pierce, *Acoustics an Introduction to its Physical Principles and Applications* (Springer Nature Switzerland AG, Cham, Switzerland, 2019).
[33] R. Snodgrass, V. Kotsubo, and J. Ullom, Comparison of three methods for oscillating flow measurements in cryocoolers, Cryocoolers **23**, 155 (2024).
[34] J. Höhne, Low frequency Stirling operation of a two-stage 4K cryocooler without rotary valve with a metal bellows compressor, Cryocoolers **22**, 255 (2022).
[35] J. Höhne, Enhancing low-frequency Stirling cryocooler efficiency with linear metal bellows compressors, Cryocoolers **23**, 193 (2024).
[36] J. Höhne, High efficiency operation of a 4K-Gifford-McMahon cryocooler without rotary valve with a metal bellows compressor, IOP Conf. Ser.: Mater. Sci. Eng. **1301**, 012142 (2024).
[37] M. Lazo, R. Galvez, R. Rogers, H. Solis, E. Tapia, D. Maltes, P. Collins, J. White, C. Cavedoni, C. Yamasaki *et al.*, Gemini helium closed cycle cooling system, in *Ground-Based and Airborne Instrumentation for Astronomy II* (2008), Vol. 7014, pp. 2527–2536.